Planet. Space Sci., Vol. 30, No. 10, pp. 999–1006, 1982
Printed in Great Britain.

0032-0633/82/100999-08$03.00/0
Pergamon Press Ltd.

ENERGETIC PARTICLE LOSSES AND TRAPPING BOUNDARIES AS DEDUCED FROM CALCULATIONS WITH A REALISTIC MAGNETIC FIELD MODEL

V. A. SERGEEV and N. A. TSYGANENKO
Institute of Physics, Leningrad State University, Leningrad 198904, U.S.S.R.

(*Received in final form* 1 *March* 1982)

Abstract—An interpretation of the stable trapping boundaries of energetic electrons and protons during quiet periods is given basing on a realistic magnetospheric magnetic field model. Particle losses are explained in terms of an ionospheric and drift loss cone filling due to a non-adiabatic pitch-angle scattering in the nightside magnetotail current sheet. The proposed mechanism is shown to provide a good agreement of the observed and calculated positions of the energetic particle trapping boundaries, as well as their energy dependence. The obtained results can be applied as a tool for investigating the magnetospheric magnetic field structure using the particle data of low-altitude satellites.

1. INTRODUCTION

Unlike the low-energy plasma, the motion of energetic particles with energies $w \geq 100$ keV is governed mainly by the magnetic field. In the region of the outer radiation belt ($r > 3$–5 *Re*) the Earth's magnetic field is distorted significantly by the currents flowing at the magnetopause and in the near-equatorial zone (plasma sheet and the ring current). This results in several important peculiarities of the particle dynamics, including the drift-shell splitting and losses of particles outside the stable trapping region (Roederer, 1970), as well as the pitch-angle scattering of particles in the regions where their motion is not fully adiabatic (Taylor and Hastie, 1971). Following the pioneering work of Williams and Mead (1965), many authors had studied different aspects of the evolution of high-energy particle fluxes and the possibility to use them as tracers of the distorted magnetospheric field. At this stage, however, the main success was achieved in the interpretation of solar particles (see review of Morfill and Scholer, 1973). At the same time, the vast amount of information on radiation belt particles obtained by low-altitude satellites was not used properly to obtain quantitative information on the changes of the geomagnetic field in the near-Earth region of the magnetosphere. Moreover, the interpretation of important features of particle population in the outer radiation belt, such as the trapping and isotropy boundaries, as well as zones of intense particle precipitation, is unclear and controversial in many respects. Application of this extensive information to studies of dynamical changes in the magnetospheric field presents a difficult but attractive problem.

Spatial distribution of the high-energy particles depends in a complicated way on the temporal evolution of several factors, including the source of fresh energetic particles, their transport and energization, particle losses and changes of the magnetic field. In a number of situations it is difficult to distinguish between these factors and to extract information on the instantaneous configuration of the geomagnetic field. The best example is the expansion phase of the magnetospheric substorm, when the particle acceleration and injection processes operate intermittently in different parts of the magnetotail plasma sheet (Krimigis and Sarris, 1979; Baker *et al.*, 1979), growing ULF–VLF noise enhances the pitch-angle and radial diffusion of particles, rapid and strong changes are observed also in the magnetic field (Russell and McPherron, 1973). An opposite situation seems to be the case during a prolonged quiet period, when the source of energetic particles appears to be weak or even absent at all, the ULF–VLF waves are much weaker, as compared to the disturbed periods and no significant changes are observed in the magnetospheric magnetic field. In such a situation the influence of magnetospheric structure on particle flux distribution in the radiation belts seems to be the most direct and distinct.

Our study is devoted to a model calculation with the aim to obtain the drift shells, particle losses, boundaries of stable trapping and precipitation of radiation belt particles, following only from the properties of a quiet-time magnetospheric magnetic field. A reasonable agreement of the calculated parameters and those obtained from the experiment during quiet times (such as the day–night asymmetry of the particle fluxes and trapping boundaries, peculiarities of particle precipitation at the night side) lend a strong support to our suggestion, that in such situations the structure of the magnetospheric field is a principal factor controlling the radiation belt particle fluxes.

An especially interesting question is the role of the real magnetic field configuration in the particle losses and precipitation. Up to date, in most studies of the low-altitude data the particle precipitation has been interpreted exclusively as a result of the collective interactions and particle scattering by the ULF–VLF waves (see e.g. a recent paper by Hultqvist, 1980). At the same time, a particle can experience a significant pitch-angle scattering because of the violation of the first adiabatic invariant, particularly inside of thin current sheet in the near-equatorial part of the magnetotail (see Taylor and Hastie, 1971 and more detailed studies by Wagner *et al.*, 1979 and Tsyganenko, 1981). An important role of this mechanism at the night side of the magnetosphere has been verified by recent experimental results of West *et al.* (1978b) and Imhof *et al.* (1979). Our purpose here is to consider this process in more detail in the real magnetospheric configuration with application to the low-altitude measurements of energetic particles and to estimate the rate of particle losses.

2. A MAGNETOSPHERIC MAGNETIC FIELD MODEL

We have used a version of the semi-empirical quantitative model of Tsyganenko (1979), pertinent to the quiet conditions. The principles of the development of this model as well as its comparison with other quantitative models and experimental data are described in detail by Sergeev and Tsyganenko (1980) and by Tsyganenko (1981). One of the essential advantages of the model is the most accurate representation of the magnetic field distribution in the near-equatorial region, which is of great importance for our purposes. Also, the model does not contain unreally abrupt field reversals and non-physical singularities as well.

The main parameters of the used model version are as follows: the subsolar magnetopause distance $R_s = 11.4\ Re$, the maximum magnetotail current density corresponds to equivalent magnetic field just above the current sheet $B_T = 43$ nT; the maximum is located at $r = 8\ Re$ (Fig. 1a); the half-thickness of the equatorial current sheet is $1\ Re$. Recent results of West *et al.* (1978a) have shown that the degree of field line stretching at the night side and the current density in the equatorial current sheet are significantly variable during quiet conditions ($A_E < 100$ nT, $K_p = 0$–1). As a parameter specifying the current intensity, they had used the field value in the tail lobe at $x = -15\ Re$, which quantity was found to vary within the range 15–30 nT. In our case the corresponding model field magnitude at this distance is 28 nT; the model corresponds thus to the quiet state of the magnetotail with a high degree of the field line stretching. The ionospheric projection of the point located at $r = 16.5\ Re$ in the midnight equatorial region, which corresponds to the last closed drift shell for particles mirroring at ionospheric heights, has in our model the latitude $\Lambda = 68.5°$.

Using this model, we have calculated the following parameters necessary for studying the particle motion and losses: the second adiabatic invariant (I), the net length of particle trajectory between mirror points (S_b), bounce (τ_b) and drift (τ_D) periods, ionospheric (α_i) and drift (α_D) loss cones, radius of the field line curvature at the equator (R_c) and so on. (Roederer's (1970) notations are used for all quantities). Variation of several important parameters along the x-axis at the night side of the model magnetosphere are shown in Fig. 1.

Some words must be said about the comparison with the particle data obtained near the ionosphere. In view of large variation of the current magnitude in the equatorial magnetospheric region and hence, of the corresponding extent of the field line stretching, the ionospheric projection of a fixed equatorial point may exhibit a significant displacement. A quantitative study of this question by using the model versions with different current intensity has shown that the change in the current only by 30% leads to the latitudinal shift of the field line foot of the order $\sim 1°$. Since the magnetospheric conditions, corresponding to the published data, are not known exactly and the current variation during quiet conditions is significant, there exists an uncertainty in comparisons of calculated and observed particle flux features. Moreover, the exact position of the field line foot depends on the geodipole tilt angle, the difference

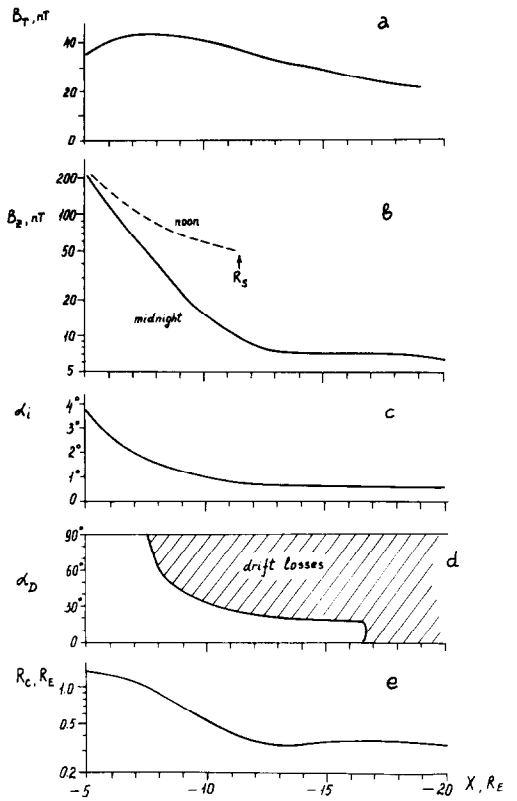

FIG. 1. RADIAL DEPENDENCE OF SEVERAL MODEL PARAMETERS: (a) VARIATION OF LINEAR CURRENT DENSITY IN THE EQUATORIAL CURRENT SHEET EXPRESSED IN UNITS OF EQUIVALENT MAGNETIC FIELD B_T, (b) B_z COMPONENT OF MAGNETIC FIELD AT THE EQUATOR, (c) ANGULAR WIDTH OF THE IONOSPHERIC LOSS CONE, (d) ANGULAR WIDTH OF THE DRIFT LOSS CONE; HATCHING CORRESPONDS TO THE REGION, WHERE THE PARTICLE CAN NOT COMPLETE ITS DRIFT REVOLUTION, (e) RADIUS OF THE FIELD LINE CURVATURE AT THE EQUATOR.

All the values correspond to the night side equatiorial magnetosphere (along the Sun–Earth line), with exception of broken line in Fig. 1b, giving the B_z-component at the day side.

in latitudes of conjugate points at solstices being about 0.5–1° in the nightside auroral zone and as large as 3° at the dayside around $\Lambda = 70°$ (Sergeev and Tsyganenko, 1980). Bearing in mind all these considerations, we feel that the main attention should be paid to the explanation of the gross features of the quiet time particle data and a discrepancy between the calculated and observed location of trapping or isotropy boundaries can be as high as $\sim 1°$ in latitude. By the last reason, the main results of our model calculations (Figs. 1, 4) are presented vs the field line equatorial radius (calculations were made for the case of zero geodipole tilt angle), rather than against the invariant latitude at the ionospheric level.

3. DRIFT SHELLS AND THE CONE OF DRIFT LOSSES

The result of calculation of the adiabatic drift shells (I, B_m = const) for particles, mirroring at the height 400 km above the Earth's surface, is shown in Fig. 2 for the noon–midnight meridian plane. The experimental points are shown also, characterizing the day–night asymmetry of the high energy electron fluxes (from Williams and Mead, 1965), the average position of the trapping boundary for $w > 40$ keV electrons (Rossberg, 1978) and that for 100–200 keV protons (Lindalen *et al.*, 1971). All these data are pertinent to quiet periods. The agreement between the model and experimental data is reasonably good; at higher latitudes ($\Lambda_D > 70°$) the day–night asymmetry in the model seems to be slightly greater (by $\sim 1°$) than that deduced experimentally.

Existence of the pseudo-trapping region at the nightside (hatched area in Fig. 1d) is a consequence of small field values inside the tail current sheet. Before reaching the noon meridian plane, the drift trajectories of near-equatorial particles approach the magnetopause, which is a perfect absorber of energetic particles (Williams *et al.*, 1979).

Contrary to the earlier studies (Roederer, 1970; Morfill and Scholer, 1973), the pseudo-trapping region at high latitudes in the day sector is absent in our case, since the field lines at the night side are closed everywhere across the current sheet in our model (and in reality, too). The appearance of

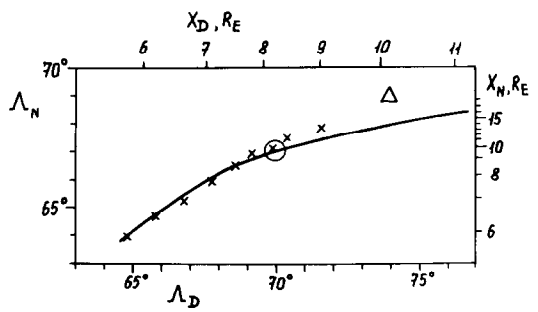

FIG. 2. SOLID CURVE SHOWS THE IONOSPHERIC PROJECTION LATITUDES OF ADIABATIC DRIFT SHELLS AT NOON–MIDNIGHT PLANE AT THE DAY SIDE (Λ_D) AND NIGHT SIDE (Λ_N); ALSO THE CORRESPONDING EQUATORIAL DISTANCES ARE GIVEN.

Crosses, triangles and open circles are experimental points obtained from the low-altitude measurements by Williams and Mead (1965), Rossberg (1978) and Lindalen *et al.* (1971), respectively.

this region in the earlier studies is thus an artificial feature, which had arised due to an over-simplified modeling of the equatorial current sheet.

4. PITCH-ANGLE SCATTERING OF PARTICLES

If the Larmor parameter $\rho = mvc/eB$ (v being the total particle velocity) becomes comparable to the radius of the field line curvature in the equatorial current sheet, then the first adiabatic invariant is violated and the pitch-angle scattering of particles occurs. This mechanism appears to play a significant role in the nightside magnetosphere even during quiet periods. We summarize below the results of a numerical study of particle scattering in the current sheet (Tsyganenko, 1981), with the emphasis on behaviour of the particles mirroring at ionospheric heights.

The data presented in Fig. 3 show the standard deviation of the final pitch angle distribution of the near-Earth mirroring particles as a function of the ratio R_c/ρ. Each point has been calculated by means of numerical tracing of 300 trajectories of particles having their initial pitch angles being distributed within a small interval $\Delta\theta = 0.1°$ around the value $\theta_o = 2.0°$ and with a uniform distribution in the gyrophase. The calculations comprise a number of models with different values of the ratio B_T/B_z, where B_T is the magnetic field outside the reversal region and B_z is the field component across the sheet, as well as for different values of the dimensionless current sheet thickness $\beta = d/\rho$.

The $\Delta\theta$ curve plotted in Fig. 3 shows that the pitch angle scattering increases when the ratio R_c/ρ falls below 10. For $R_c/\rho \lesssim 3$ the dispersion value ($\Delta\theta$) exceeds 10° (see Wagner *et al.*, 1979; Tsyganenko, 1981) and hence, complete pitch-angle mixing in the final distribution is achieved in this case after several crossings of the field reversal region.

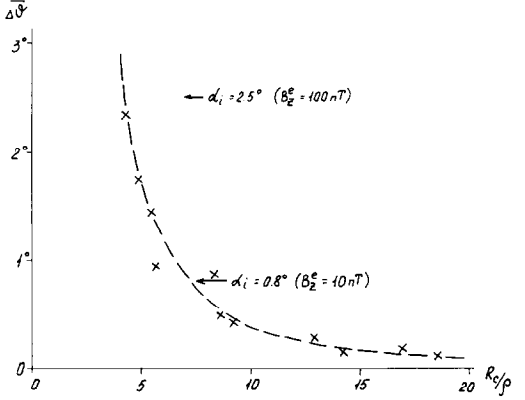

FIG. 3. THE R_c/ρ DEPENDENCE OF THE AVERAGE CHANGE IN THE PARTICLE PITCH ANGLE (ABSOLUTE VALUE) AFTER ONE CROSSING OF THE FIELD REVERSAL REGION; $\Delta\theta$ CORRESPONDS TO THE STANDARD DEVIATION OF THE EQUATORIAL PITCH ANGLE.

As for the conditions of isotropic particle precipitation into the ionosphere (i.e. when $\Delta\theta \geq \alpha_i$), we have found a slight dependence of the 'critical' value of R_c/ρ on the width of the ionospheric loss cone α_i, defined by the value of B_z. Thus, for $B_z = 10$ nT the condition $\Delta\theta = \alpha_i$ corresponds to $R_c/\rho \approx 7$; respectively, for $B_z = 100$ nT we have obtained $R_c/\rho \approx 4.5$ (see Fig. 3). Therefore, we can use the curves $B\cdot\rho = 0.1\ R_cB_z$ and $= 0.2\ R_cB_z$, shown in Fig. 4a, as an approximate criterion of the innermost boundary of isotropic precipitation. As was pointed out above, the Larmor parameter is calculated by substitution of the total velocity of energetic particle and therefore, the quantity B_ρ is constant for a given particle along the field line and corresponds well to the rigidity of trapped particles measured at low altitudes.

The circles in Fig. 4a denote the equatorial position of the innermost boundary of isotropic particle fluxes for different rigidities, obtained from measurements of magnetic field and energetic particles in the near-equatorial region at OGO-5 satellite on August 2, 1968 (West *et al.*, 1978b). The experimental points $B\rho(x)$ behave similarly to the curves $R_cB_z = \text{const.}$ obtained from our model calculations, showing, however, an even more steep spatial gradient. This event (the only one, for which West *et al.* (1978b) had presented the data in a form convenient for comparison) corresponds to the most tail-like case of the all quiet-time data. This feature can reflect a somewhat more intense current and/or smaller B_z-component at the equator during the period of measurements.

5. RATE OF PARTICLE LOSSES

Under assumption of the strong pitch-angle scattering of particles, which really takes place even in the quiet-time nightside magnetosphere, we can obtain a reasonable estimate of particle loss rate without a rigorous treatment of the particle diffusion problem. If the $\Delta\theta \geq \alpha_i$ condition is satisfied, then the particles fill the whole ionospheric loss cone after the first crossing of the equatorial reversal region and the characteristic time scale of particle losses in the flux tube can be evaluated as (Kennel, 1969): $T_i = \tau_b/2\alpha_i^2$. The values of T_i at the midnight for electrons and protons with $w = 100$ keV are shown in Fig. 4b.

Along with the losses of particles because of

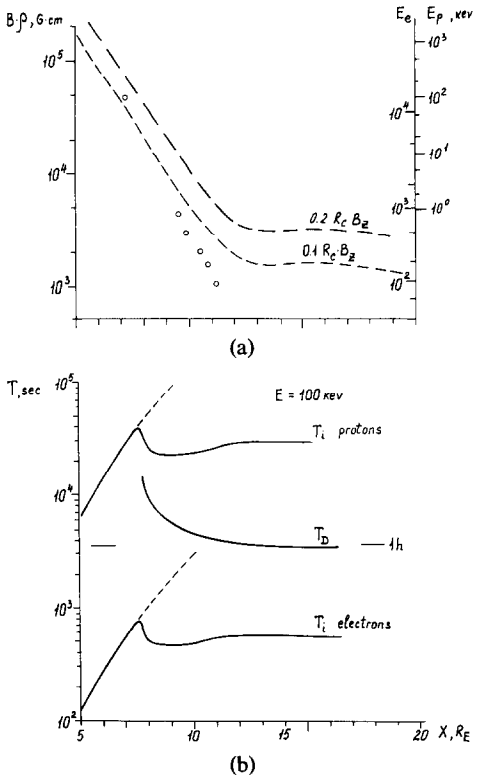

FIG. 4. (a) THE INNERMOST BOUNDARY OF THE STRONG PITCH-ANGLE SCATTERING FOR PARTICLES OF DIFFERENT RIGIDITIES AT THE NIGHT SIDE; BROKEN LINE REFERS TO THE MODEL CALCULATIONS, OPEN CIRCLES ARE EXPERIMENTAL POINTS BY WEST *et al.* (1978), (b) PLOTS OF CHARACTERISTIC LOSS TIMES OF 100 keV PROTONS AND ELECTRONS DUE TO THEIR PRECIPITATION INTO IONOSPHERE (T_i) AND THAT CORRESPONDING TO SCATTERING INTO THE DRIFT LOSS CONE (T_D), VS THE RADIAL DISTANCE OF THE DRIFT SHELL AT THE MIDNIGHT EQUATOR.

These estimates of loss times are applicable only in the flux tubes, where a strong non-adiabatic scattering occurs (compare with Fig. 4a).

their precipitation into the ionosphere, another loss mechanism operates at distances $r > 7.5\ Re$ at the night side, where the drift shells of near-equatorial particles are not closed, intersecting with the magnetopause. To our knowledge, this mechanism was not discussed as yet in the literature; however, it appears to be very effective on those drift shells, where a strong scattering occurs and at the same time, the drift loss cone does exist. If particles, drifting in the nightside region, have enough time to be scattered isotropically, then their part contained in the drift loss cone will be lost. The factor $\delta = \cos\alpha_D/(1-\cos\alpha_D)$ can be introduced, representing the ratio of the drift loss cone solid angle to that outside the cone. At geocentric distances $r \sim 10$–$16\ Re$ in the tail α_D is of the order $\sim 20°$–$30°$ and hence, the factor $\delta \sim 10$. Therefore, a significant part of the particle population will be lost after one drift period τ_D. By analogy with the Kennel's estimate for the ionospheric losses, we can define the time scale of drift losses as $T_D = \tau_D/\cos\alpha_D$, which is applicable after averaging of losses over one drift period. The value of τ_D was calculated from the above mentioned model along the drift shell of the near-Earth-mirroring particles by the method outlined in Appendix 3 of Roederer's (1970) book. The curve for the loss time T_D is also plotted in Fig. 4b for the particles, having the same energy $w = 100$ keV. The drift losses dominate for energetic protons, having very large values of T_i. For energetic electrons we also have $T_D < T_i$ at distances $r > 11\ Re$, but only at these distances the strong pitch-angle scattering takes place. Bearing in mind, that with the increase of particle energy T_D decreases more rapidly (as w^{-1}) than T_i (which is proportional to the inverse of particle velocity, i.e. as $w^{-1/2}$) we find, that the drift losses dominate for all energetic particle population with $w \geqslant 100$ keV.

The above estimates for T_D are valid only if a sufficient number of crossings of the current sheet occurs during the particle drift across the nightside region, to fill the drift loss cone. Estimating the time necessary to cross the scattering zone as $\tau_D/4$, we obtain the number of crossings as $\tau_D/2\tau_b$, which for 100 keV particles is as high as ~ 800 for electrons and ~ 20 for protons. Both the increase of particle energy, as well as increase of the drift shell equatorial radius will lead to a decrease of the number of equatorial crossings. From these estimates we feel that the rate of real drift losses for energetic electrons should be close to our results; for the protons, however, the real losses may be significantly lower. An additional analysis of this problem is necessary, which must take into account some details of the drift loss cone filling due to a small number of crossings, as well as large radial gradients of all the parameters involved.

6. DISCUSSION

In the earlier studies (Roederer, 1970; Hess, 1966) the concept of stable trapping region was introduced to specify the part of the magnetosphere, where all the drifting energetic particles can perform a full revolution around the Earth. The so-called pseudo-trapping regions correspond to

those drift shells where, due to their splitting effect, only the particles from a limited range of pitch-angles can perform a closed drift motion without being lost at the magnetopause or in the open magnetic flux tubes. This picture of stable trapping was believed to yield a comprehensive explanation of the main observed features of energetic particle dynamics by the pure effects of the gross structure of the magnetospheric magnetic field. The experimentally observed boundary of intense particle fluxes was interpreted just as a signature of the outer boundary of the stable trapping region, or in terms of the nightside boundary between open and closed field lines, which is inherent in the models of Williams and Mead (1965) type.

In the light of our results (see also Morfill, 1973) this generally accepted picture must be changed considerably. First of all, it appears that the geomagnetic field structure determines not only the division of particle drift shells into open and closed types, but also the pitch-angle scattering and losses. The last phenomenon appears to be the most effective for particles with the typical scattering time (necessary for the pitch angle to fall into the loss cone), to the order of magnitude, less or equal to their drift period. Configuration and size of the region, where the particles can be trapped during several drift periods without a significant flux decay depends, therefore, not only on particle pitch angles, but also on their energy and mass. Even if to take into account only geometrical considerations (the division of drift shells into open and closed types), our concept is, nevertheless, different from the generally accepted one (Roederer, 1970), in which the dayside pseudotrapping region is a consequence of an unreal property of the Mead–Williams' nightside model magnetosphere.

The results shown in Fig. 1d and 4a, b can serve as a guide in the interpretation of the trapping boundary at the night side, observed by low-altitude spacecraft during quiet periods. The characteristic time scale of the decrease of energetic particle flux in the loss region after 'switching off' the source of accelerated fresh particles at the late recovery phase of a substorm is of the order of several drift periods τ_D, i.e. one or two revolution periods of a low-altitude satellite. In such a situation the trapping (background) boundary of energetic electrons will correspond to the innermost of the two boundaries, which are the last closed drift shell (Fig. 1d) and the Earthward boundary of strong non-adiabatic scattering (Fig. 4b). To distinguish between these two possibilities, we have only to find the presence (or absence) of energy dependence in the position of this boundary.

As regards the energetic protons, our estimates of the particle loss rate have given only the lower limit of T_D; the real loss times can be considerably larger. In this respect it is interesting to note a sharp contrast between the proton and electron precipitation during prolonged quiet periods: whereas the electron pricipitation is absent (Rossberg, 1978), an intense precipitation of energetic protons (with approximately isotropic pitch angle distribution in the loss cone) is measured systematically at the night side (Lindalen *et al.*, 1971; Lundblad *et al.*, 1979). A natural explanation of this different behaviour can be given, taking into account a considerably longer time necessary to scatter a significant portion of protons (as compared to electrons into the ionospheric loss cone.

As one of the main conclusions of our study, we have to emphasize the significant role of the non-adiabatic particle scattering in the particle precipitation and rapid losses of the trapped radiation. Its importance is proved now by both theoretical and observational results. From a theoretical standpoint, the results of numerical calculations have shown that pitch-angle scattering becomes significant when $R_c/\rho \lesssim 5$–10 (West *et al.*, 1978b; Tsyganenko, 1981), the details of the dependence of the pitch-angle deviation on R_c/ρ being given in Fig. 3. It is well established, that a remarkable change of pitch angle (up to tens of degrees) can occur after the first crossing of the reversal region (Wagner *et al.*, 1979; Tsyganenko, 1981).

From the viewpoint of real properties of nightside magnetic field in the magnetosphere, the conditions for strong scattering are met even during quiet conditions for the wide range of particle rigidities (West *et al.*, 1978b, Fig. 4a). Note that the magnetic field modeling in the studies by West *et al.* (1978a, b) has been carried out on a basis of *in situ* near-equatorial measurements of both magnetic field and energetic particles; this approach reduces substantially the usual ambiguities in comparing model and experimental data. The observational arguments in favour of the operation of this scattering mechanism in reality follows from results of energetic particle measurements both in the magnetosphere (West *et al.*, 1978b) and at low altitudes (Soraas *et al.*, 1977; Imhof *et al.*, 1979, see also references therein). These results show, that at the night side (in the sector 18–03 MLT, according to Imhof *et al.*, 1979)

the position of the equatorward (innermost in the magnetosphere) boundary of nearly isotropic precipipitation is always dependent on particle rigidity in such a way that the low latitide limit of particle precipitation is shifted toward lower latitudes for higher rigidities. Moreover, the latitudinal spacing between the boundaries for particles of different rigidity is relatively stable, as the whole precipitation pattern moves towards the equator due to enhancement of the magnetic activity (Soraas *et al.*, 1977; Imhof *et al.*, 1979). These features are observed at different levels of geomagnetic activity, in physically different situations.

Bringing these observational features together, we feel that no doubts should exist concerning the operation of this strong scattering mechanism over a wide range of magnetospheric conditions.

An essentially different situation appears, as we turn to the question of the rapid particle scattering by means of the ULF–VLF waves. Being considered traditionally as the main (or even the only) reason of intense particle precipitation, this mechanism provides many difficulties in explaining intense isotropic precipitation, especially for high energy particles (see Ashour-Abdalla and Kennel, 1978; Hultqvist, 1980; and discussion by Imhof *et al.*, 1979).

It is of interest that the strong scattering in the current sheet can be important also for the low-energy (thermal) particles of the plasma sheet. For the protons with $w \sim 5$ keV the nightside demarcation boundary, delineating the strong scattering region from the zone of adiabatic motion is located at distance $r \approx 10$ *Re* during quiet periods, i.e. in a close vicinity of the inner edge of plasma sheet (Vasyliunas, 1968).

As we have mentioned in Section 3, the degree of the day–night asymmetry obtained from the data on the energetic particle fluxes is slightly higher in the model calculation (Fig. 2), than that derived from experiments. There are also other indications that the corresponding nightside latitudes of features, obtained from our model, are slightly lower, than those deduced in measurements. Thus, the position of the trapping boundary of 40 keV electrons at night side is at $\Lambda = 69°$ (Rossberg, 1978); in our case even the last closed drift shell is projected onto $\Lambda = 68.5°$. Also, the quiet-time location of the equatorward boundary of isotropic precipitation is at $L \sim 7$ (i.e. $\Lambda \sim 68°$) for 6 keV protons (Soraas *et al.*, 1979) and at $L = 5.8$ ($\Lambda = 65.5°$) for 400 keV protons (extrapolated to $A_E = 50$ nT conditions from Fig. 7 of Imhof *et al.*, 1979). The corresponding distances to the strong precipitation boundaries, as obtained from the upper of two curves in Fig. 4a in our model, give somewhat lower ionospheric projection latitudes 67.2° and 65.3°. We expect thus, that the current intensity in our model is somewhat higher and respectively, B_z-component at the equator in the inner magnetospheric region is slightly lower, than is typical to the average quiet period conditions. A simple decrease of the current intensity by $\lesssim 30\%$ (so that $B_T = 20$ nT at $r = 15$ *Re* in the tail) will remove most of these discrepancies. With this small correction, the magnetic field at 15 *Re* distance falls well into the range 15–30 nT, found by West *et al.* (1978a) for quiet conditions.

One more additional quantitative comparison is possible. The boundary of isotropic precipitation ($R_c/\rho = 5$) for 6 keV and 100 keV protons in our model are, respectively, at $\Lambda = 67.2°$ and $\Lambda = 66.0°$, the corresponding difference in L-values being $\Delta L = 0.7$. Soraas *et al.* (1977) have found experimentally that this difference is always within the range 0.2–0.7.

In view of some arbitrariness in the choice of the model parameters and some difficulties in its comparison with the energetic particle data, outlined in Section 1, the agreement of the calculated and measured quantities is remarkable. Thus, the used model of the magnetospheric magnetic field is well supported by energetic particle data (as well as by comparison with the existing magnetic field measurements—see Sergeev and Tsyganenko, 1980) and can serve as a starting point for investigating the dynamical changes of the magnetotail currents.

REFERENCES

Ashour-Abdalla, M. and Kennel, C. F. (1978). Diffuse auroral precipitation. *J. Geomagn. Geoelectr., Kyoto* **30**, 239.

Baker, D. N., Belian, R. D., Higbie, P. R. and Hones, E. W. (1979). High-energy magnetospheric protons and their dependence on geomagnetic and interplanetary conditions. *J. geophys. Res.* **84**, 7138.

Hultqvist, B. (1980). Magnetospheric hot plasma measurements in relation to wave-particle interactions on high-latitude magnetic field lines in *Exploration of the Polar Upper Atmosphere* (Deehr, C. S. and Holtet, J. A.), p. 367. D. Reidel, Dordrecht.

Imhof, W. L., Reagan, J. B. and Gaines, E. E. (1979). Studies of the sharply defined L dependent energy threshold for isotropy at the midnight trapping boundary. *J. geophys. Res.* **84**, 6371.

Kennel, C. F. (1969). Consequences of a magnetospheric plasma. *Rev. Geophys.* **7**, 379.

Krimigis, E. T. and Sarris, S. M. (1979). Energetic particle bursts in the Earth's magnetotail in *Dynamics of the Magnetosphere* (Akasofu, S.-I. ED.), p. 590. D. Reidel, Dordrecht.

Lindalen, H. R., Soraas, F., Aarsnes, K. and Amundsen, R. (1971). Variations in the high-latitude proton trapping boundary associated with polar magnetic substorms. *Planet. Space Sci.* **19**, 1041.

Lundblad, J. A., Soraas, F. and Aarsnes, K. (1979). Substorm morphology of > 100 keV protons. *Planet. Space Sci.* **27**, 841.

Morfill, G. (1973). Nonadiabatic particle motion in the magnetosphere *J. geophys. Res.* **78**, 588.

Morfill, G. and Scholer, M. (1973). Study of the magnetosphere using energetic solar particles. *Space Sci. Revs.* **15**, 267.

Roederer, J. G. (1970). Dynamics of geomagnetically trapped radiation in *Physics and Chemistry in Space*, Vol. 2, Springer, New York.

Rossberg, L. (1978). Undisturbed trapping boundary for energetic electrons at low altitudes. *J. geophys. Res.* **83**, 4307.

Russell, C. T. and McPherron, R. L. (1973). The magnetotail and substorms. *Space Sci. Revs.* **15**, 205.

Sergeev, V. A. and Tsyganenko, N. A. (1980). *The Earth's Magnetosphere.* Nauka, Moscow.

Soraas, F., Lundblad, J. A. and Hultqvist, B. (1977). On the energy dependence of the ring current proton precipitation. *Planet. Space Sci.* **25**, 757.

Taylor, H. E. and Hastie, R. J. (1971). Nonadiabatic behaviour of radiation belt particles. *Cosmic Electrodyn.* **2**, 211.

Tsyganenko, N. A. (1979). *Subroutines and tables for calculation of the geomagnetic field*, WDC-B2 issue. Moscow.

Tsyganenko, N. A. (1981). Numerical models of quiet and disturbed geomagnetic field in the cislunar part of the magnetosphere. *Ann. Geophys.* **37**, 381.

Tsyganenko, N. A. (1982). Pitch-angle scattering of energetic particles in the current sheet of the magnetospheric tail and stationary distribution functions. *Planet. Space Sci.* **30**, 433–437.

Vasyliunas, V. M. (1968). A survey of low-energy electrons in the evening sector of the magnetosphere with OGO-1 and -3. *J. geophys. Res.* **73**, 2839.

Wagner, J. S., Kan, J. R. and Akasofu, S.-I. (1979). Particle dynamics in the plasma sheet. *J. geophys. Res.* **84**, 891.

West, H. I., Buck, R. M. and Kivelson, M. G. (1978a). On the configuration of the magnetotail near midnight during quiet and weakly disturbed periods: state of the magnetosphere. *J. geophys. Res.* **83**, 3805.

West, H. I., Buck, R. M. and Kivelson, M. G. (1978b). On the configuration of the magnetotail near midnight during quiet and weakly disturbed periods: magnetic field modeling. *J. geophys. Res.* **83**, 3819.

Williams, D. J. and Mead, G. D. (1965). Nightside magnetosphere configuration as obtained from trapped electrons at 1100 km. *J. geophys. Res.* **70**, 3017.

Williams, D. J., Fritz, T. A., Wilken, B. and Keppler, E. (1979). An energetic particle perspective of the magnetopause. *J. geophys. Res.* **84**, 6385.